

Measurement of J/ψ Azimuthal Anisotropy in Au+Au Collisions at $\sqrt{s_{NN}} = 200$ GeV

L. Adamczyk,¹ J. K. Adkins,²³ G. Agakishiev,²¹ M. M. Aggarwal,³⁴ Z. Ahammed,⁵³ I. Alekseev,¹⁹ J. Alford,²² C. D. Anson,³¹ A. Aparin,²¹ D. Arkhipkin,⁴ E. Aschenauer,⁴ G. S. Averichev,²¹ J. Balewski,²⁶ A. Banerjee,⁵³ Z. Barnovska,¹⁴ D. R. Beavis,⁴ R. Bellwied,⁴⁹ M. J. Betancourt,²⁶ R. R. Betts,¹⁰ A. Bhasin,²⁰ A. K. Bhati,³⁴ Bhattarai,⁴⁸ H. Bichsel,⁵⁵ J. Bielcik,¹³ J. Bielcikova,¹⁴ L. C. Bland,⁴ I. G. Bordyuzhin,¹⁹ W. Borowski,⁴⁵ J. Bouchet,²² A. V. Brandin,²⁹ S. G. Brovko,⁶ E. Bruna,⁵⁷ S. Bültmann,³² I. Bunzarov,²¹ T. P. Burton,⁴ J. Butterworth,⁴⁰ X. Z. Cai,⁴⁴ H. Caines,⁵⁷ M. Calderón de la Barca Sánchez,⁶ D. Cebra,⁶ R. Cendejas,³⁵ M. C. Cervantes,⁴⁷ P. Chaloupka,¹³ Z. Chang,⁴⁷ S. Chattopadhyay,⁵³ H. F. Chen,⁴² J. H. Chen,⁴⁴ J. Y. Chen,⁹ L. Chen,⁹ J. Cheng,⁵⁰ M. Cherney,¹² A. Chikanian,⁵⁷ W. Christie,⁴ P. Chung,¹⁴ J. Chwastowski,¹¹ M. J. M. Codrington,⁴⁸ R. Corliss,²⁶ J. G. Cramer,⁵⁵ H. J. Crawford,⁵ X. Cui,⁴² S. Das,¹⁶ A. Davila Leyva,⁴⁸ L. C. De Silva,⁴⁹ R. R. Debbe,⁴ T. G. Dedovich,²¹ J. Deng,⁴³ R. Derradi de Souza,⁸ S. Dhamija,¹⁸ B. di Ruzza,⁴ L. Didenko,⁴ F. Ding,⁶ A. Dion,⁴ P. Djawotho,⁴⁷ X. Dong,²⁵ J. L. Drachenberg,⁵² J. E. Draper,⁶ C. M. Du,²⁴ L. E. Dunkelberger,⁷ J. C. Dunlop,⁴ L. G. Efimov,²¹ M. Elnimr,⁵⁶ J. Engelage,⁵ G. Eppley,⁴⁰ L. Eun,²⁵ O. Evdokimov,¹⁰ R. Fatemi,²³ S. Fazio,⁴ J. Fedorisin,²¹ R. G. Fersch,²³ P. Filip,²¹ E. Finch,⁵⁷ Y. Fisyak,⁴ E. Flores,⁶ C. A. Gagliardi,⁴⁷ D. R. Gangadharan,³¹ D. Garand,³⁷ F. Geurts,⁴⁰ A. Gibson,⁵² S. Gliske,² O. G. Grebenyuk,²⁵ D. Grosnick,⁵² A. Gupta,²⁰ S. Gupta,²⁰ W. Guryn,⁴ B. Haag,⁶ O. Hajkova,¹³ A. Hamed,⁴⁷ L.-X. Han,⁴⁴ J. W. Harris,⁵⁷ J. P. Hays-Wehle,²⁶ S. Heppelmann,³⁵ A. Hirsch,³⁷ G. W. Hoffmann,⁴⁸ D. J. Hofman,¹⁰ S. Horvat,⁵⁷ B. Huang,⁴ H. Z. Huang,⁷ P. Huck,⁹ T. J. Humanic,³¹ G. Igo,⁷ W. W. Jacobs,¹⁸ C. Jena,³⁰ E. G. Judd,⁵ S. Kabana,⁴⁵ K. Kang,⁵⁰ J. Kapitan,¹⁴ K. Kauder,¹⁰ H. W. Ke,⁹ D. Keane,²² A. Kechechyan,²¹ A. Kesich,⁶ D. P. Kikola,³⁷ J. Kiryluk,²⁵ I. Kisel,²⁵ A. Kisiel,⁵⁴ S. R. Klein,²⁵ D. D. Koetke,⁵² T. Kollegger,¹⁵ J. Konzer,³⁷ I. Koralt,³² W. Korsch,²³ L. Kotchenda,²⁹ P. Kravtsov,²⁹ K. Krueger,² I. Kulakov,²⁵ L. Kumar,²² M. A. C. Lamont,⁴ J. M. Landgraf,⁴ K. D. Landry,⁷ S. LaPointe,⁵⁶ J. Lauret,⁴ A. Lebedev,⁴ R. Lednicky,²¹ J. H. Lee,⁴ W. Leight,²⁶ M. J. LeVine,⁴ C. Li,⁴² W. Li,⁴⁴ X. Li,³⁷ X. Li,⁴⁶ Y. Li,⁵⁰ Z. M. Li,⁹ L. M. Lima,⁴¹ M. A. Lisa,³¹ F. Liu,⁹ T. Ljubicic,⁴ W. J. Llope,⁴⁰ R. S. Longacre,⁴ Y. Lu,⁴² X. Luo,⁹ A. Luszczak,¹¹ G. L. Ma,⁴⁴ Y. G. Ma,⁴⁴ D. M. M. D. Madagodagettige Don,¹² D. P. Mahapatra,¹⁶ R. Majka,⁵⁷ S. Margetis,²² C. Markert,⁴⁸ H. Masui,²⁵ H. S. Matis,²⁵ D. McDonald,⁴⁰ T. S. McShane,¹² S. Mioduszewski,⁴⁷ M. K. Mitrovski,⁴ Y. Mohammed,⁴⁷ B. Mohanty,³⁰ M. M. Mondal,⁴⁷ M. G. Munhoz,⁴¹ M. K. Mustafa,³⁷ M. Naglis,²⁵ B. K. Nandi,¹⁷ Md. Nasim,⁵³ T. K. Nayak,⁵³ J. M. Nelson,³ L. V. Nogach,³⁶ J. Novak,²⁸ G. Odyniec,²⁵ A. Ogawa,⁴ K. Oh,³⁸ A. Ohlson,⁵⁷ V. Okorokov,²⁹ E. W. Oldag,⁴⁸ R. A. N. Oliveira,⁴¹ D. Olson,²⁵ M. Pachr,¹³ B. S. Page,¹⁸ S. K. Pal,⁵³ Y. X. Pan,⁷ Y. Pandit,¹⁰ Y. Panebratsev,²¹ T. Pawlak,⁵⁴ B. Pawlik,³³ H. Pei,¹⁰ C. Perkins,⁵ W. Peryt,⁵⁴ P. Pile,⁴ M. Planinic,⁵⁸ J. Pluta,⁵⁴ N. Poljak,⁵⁸ J. Porter,²⁵ A. M. Poskanzer,²⁵ C. B. Powell,²⁵ C. Pruneau,⁵⁶ N. K. Pruthi,³⁴ M. Przybycien,¹ P. R. Pujahari,¹⁷ J. Putschke,⁵⁶ H. Qiu,²⁵ S. Ramachandran,²³ R. Raniwala,³⁹ S. Raniwala,³⁹ R. L. Ray,⁴⁸ C. K. Riley,⁵⁷ H. G. Ritter,²⁵ J. B. Roberts,⁴⁰ O. V. Rogachevskiy,²¹ J. L. Romero,⁶ J. F. Ross,¹² L. Ruan,⁴ J. Rusnak,¹⁴ N. R. Sahoo,⁵³ P. K. Sahu,¹⁶ I. Sakrejda,²⁵ S. Salur,²⁵ A. Sandacz,⁵⁴ J. Sandweiss,⁵⁷ E. Sangaline,⁶ A. Sarkar,¹⁷ J. Schambach,⁴⁸ R. P. Scharenberg,³⁷ A. M. Schmah,²⁵ B. Schmidke,⁴ N. Schmitz,²⁷ T. R. Schuster,¹⁵ J. Seger,¹² P. Seyboth,²⁷ N. Shah,⁷ E. Shahaliev,²¹ M. Shao,⁴² B. Sharma,³⁴ M. Sharma,⁵⁶ S. S. Shi,⁹ Q. Y. Shou,⁴⁴ E. P. Sichtermann,²⁵ R. N. Singaraju,⁵³ M. J. Skoby,¹⁸ D. Smirnov,⁴ N. Smirnov,⁵⁷ D. Solanki,³⁹ P. Sorensen,⁴ U. G. deSouza,⁴¹ H. M. Spinka,² B. Srivastava,³⁷ T. D. S. Stanislaus,⁵² J. R. Stevens,²⁶ R. Stock,¹⁵ M. Strikhanov,²⁹ B. Stringfellow,³⁷ A. A. P. Suaide,⁴¹ M. C. Suarez,¹⁰ M. Sumbera,¹⁴ X. M. Sun,²⁵ Y. Sun,⁴² Z. Sun,²⁴ B. Surrow,⁴⁶ D. N. Svirida,¹⁹ T. J. M. Symons,²⁵ A. Szanto de Toledo,⁴¹ J. Takahashi,⁸ A. H. Tang,⁴ Z. Tang,⁴² L. H. Tarini,⁵⁶ T. Tarnowsky,²⁸ J. H. Thomas,²⁵ J. Tian,⁴⁴ A. R. Timmins,⁴⁹ D. Tlusty,¹⁴ M. Tokarev,²¹ S. Trentalange,⁷ R. E. Tribble,⁴⁷ P. Tribedy,⁵³ B. A. Trzeciak,⁵⁴ O. D. Tsai,⁷ J. Turnau,³³ T. Ullrich,⁴ D. G. Underwood,² G. Van Buren,⁴ G. van Nieuwenhuizen,²⁶ J. A. Vanfossen, Jr.,²² R. Varma,¹⁷ G. M. S. Vasconcelos,⁸ F. Videbæk,⁴ Y. P. Viyogi,⁵³ S. Vokal,²¹ S. A. Voloshin,⁵⁶ A. Vossen,¹⁸ M. Wada,⁴⁸ F. Wang,³⁷ G. Wang,⁷ H. Wang,⁴ J. S. Wang,²⁴ Q. Wang,³⁷ X. L. Wang,⁴² Y. Wang,⁵⁰ G. Webb,²³ J. C. Webb,⁴ G. D. Westfall,²⁸ C. Whitten Jr.,⁷ H. Wieman,²⁵ S. W. Wissink,¹⁸ R. Witt,⁵¹ Y. F. Wu,⁹ Z. Xiao,⁵⁰ W. Xie,³⁷ K. Xin,⁴⁰ H. Xu,²⁴ N. Xu,²⁵ Q. H. Xu,⁴³ W. Xu,⁷ Y. Xu,⁴² Z. Xu,⁴ L. Xue,⁴⁴ Y. Yang,²⁴ Y. Yang,⁹ P. Yepes,⁴⁰ L. Yi,³⁷ K. Yip,⁴ I.-K. Yoo,³⁸ M. Zawisza,⁵⁴ H. Zbroszczyk,⁵⁴ J. B. Zhang,⁹ S. Zhang,⁴⁴ X. P. Zhang,⁵⁰ Y. Zhang,⁴² Z. P. Zhang,⁴² F. Zhao,⁷ J. Zhao,⁴⁴ C. Zhong,⁴⁴ X. Zhu,⁵⁰ Y. H. Zhu,⁴⁴ Y. Zoukarneeva,²¹ and M. Zyzak²⁵

(STAR Collaboration)

- ¹AGH University of Science and Technology, Cracow, Poland
²Argonne National Laboratory, Argonne, Illinois 60439, USA
³University of Birmingham, Birmingham, United Kingdom
⁴Brookhaven National Laboratory, Upton, New York 11973, USA
⁵University of California, Berkeley, California 94720, USA
⁶University of California, Davis, California 95616, USA
⁷University of California, Los Angeles, California 90095, USA
⁸Universidade Estadual de Campinas, Sao Paulo, Brazil
⁹Central China Normal University (HZNU), Wuhan 430079, China
¹⁰University of Illinois at Chicago, Chicago, Illinois 60607, USA
¹¹Cracow University of Technology, Cracow, Poland
¹²Creighton University, Omaha, Nebraska 68178, USA
¹³Czech Technical University in Prague, FNSPE, Prague, 115 19, Czech Republic
¹⁴Nuclear Physics Institute AS CR, 250 68 Řež/Prague, Czech Republic
¹⁵University of Frankfurt, Frankfurt, Germany
¹⁶Institute of Physics, Bhubaneswar 751005, India
¹⁷Indian Institute of Technology, Mumbai, India
¹⁸Indiana University, Bloomington, Indiana 47408, USA
¹⁹Alikhanov Institute for Theoretical and Experimental Physics, Moscow, Russia
²⁰University of Jammu, Jammu 180001, India
²¹Joint Institute for Nuclear Research, Dubna, 141 980, Russia
²²Kent State University, Kent, Ohio 44242, USA
²³University of Kentucky, Lexington, Kentucky, 40506-0055, USA
²⁴Institute of Modern Physics, Lanzhou, China
²⁵Lawrence Berkeley National Laboratory, Berkeley, California 94720, USA
²⁶Massachusetts Institute of Technology, Cambridge, MA 02139-4307, USA
²⁷Max-Planck-Institut für Physik, Munich, Germany
²⁸Michigan State University, East Lansing, Michigan 48824, USA
²⁹Moscow Engineering Physics Institute, Moscow Russia
³⁰National Institute of Science and Education and Research, Bhubaneswar 751005, India
³¹Ohio State University, Columbus, Ohio 43210, USA
³²Old Dominion University, Norfolk, VA, 23529, USA
³³Institute of Nuclear Physics PAN, Cracow, Poland
³⁴Panjab University, Chandigarh 160014, India
³⁵Pennsylvania State University, University Park, Pennsylvania 16802, USA
³⁶Institute of High Energy Physics, Protvino, Russia
³⁷Purdue University, West Lafayette, Indiana 47907, USA
³⁸Pusan National University, Pusan, Republic of Korea
³⁹University of Rajasthan, Jaipur 302004, India
⁴⁰Rice University, Houston, Texas 77251, USA
⁴¹Universidade de Sao Paulo, Sao Paulo, Brazil
⁴²University of Science & Technology of China, Hefei 230026, China
⁴³Shandong University, Jinan, Shandong 250100, China
⁴⁴Shanghai Institute of Applied Physics, Shanghai 201800, China
⁴⁵SUBATECH, Nantes, France
⁴⁶Temple University, Philadelphia, Pennsylvania, 19122
⁴⁷Texas A&M University, College Station, Texas 77843, USA
⁴⁸University of Texas, Austin, Texas 78712, USA
⁴⁹University of Houston, Houston, TX, 77204, USA
⁵⁰Tsinghua University, Beijing 100084, China
⁵¹United States Naval Academy, Annapolis, MD 21402, USA
⁵²Valparaiso University, Valparaiso, Indiana 46383, USA
⁵³Variable Energy Cyclotron Centre, Kolkata 700064, India
⁵⁴Warsaw University of Technology, Warsaw, Poland
⁵⁵University of Washington, Seattle, Washington 98195, USA
⁵⁶Wayne State University, Detroit, Michigan 48201, USA
⁵⁷Yale University, New Haven, Connecticut 06520, USA
⁵⁸University of Zagreb, Zagreb, HR-10002, Croatia

(Dated: December 14, 2012)

The measurement of J/ψ azimuthal anisotropy is presented as a function of transverse momentum for different centralities in Au+Au collisions at $\sqrt{s_{NN}} = 200$ GeV. The measured J/ψ elliptic flow is consistent with zero within errors for transverse momentum between 2 and 10 GeV/c. Our

measurement suggests that J/ψ with relatively large transverse momentum are not dominantly produced by coalescence from thermalized charm quarks, when comparing to model calculations.

PACS numbers: 25.75.Cj, 12.38.Mh, 14.40.Pq

Quantum chromodynamics (QCD) predicts a quark-gluon plasma (QGP) phase at extremely high temperature and/or density, consisting of deconfined quarks and gluons. Over the past twenty years, heavy quarkonia production in hot and dense nuclear matter has been a topic attracting growing interest. In relativistic heavy-ion collisions the $c\bar{c}$ bound state is subject to dissociation due to the color screening and the change of binding potential in the deconfined medium. As a consequence, the production of J/ψ is expected to be suppressed, and such suppression has been proposed as a signature of QGP formation [1]. However, the J/ψ suppression observed in experiments [2–6] can also be affected by additional cold [7, 8] and hot [9–14] nuclear effects. In particular the recombination of J/ψ from a thermalized charm quark and its antiquark has not been unambiguously established experimentally [11–14]. By measuring J/ψ azimuthal anisotropy, especially its second Fourier coefficient v_2 (elliptic flow), one may disentangle J/ψ from direct pQCD processes and from recombination. J/ψ produced from direct pQCD processes, which do not have initial collective motion, should have little azimuthal preference. In non-central collisions, the produced J/ψ will then gain limited azimuthal anisotropy from azimuthally different absorption due to the different path lengths in azimuth. On the other hand, J/ψ produced from recombination of thermalized charm quarks will inherit the flow of charm quarks, exhibiting considerable flow.

Many models that describe the experimental results of heavy-ion collisions depend on the assumption that light flavor quarks in the medium reach thermalization on a short timescale (~ 0.5 fm/c) [15, 16]. However, the dynamics through which the rapid thermalization happens, are not very clear, and it has not been established to what extent thermalization applies. The flow pattern of heavy quarks provides a unique tool to test the thermalization. With much larger mass than that of light quarks, heavy quarks are more resistant to having their velocity changed, and are thus expected to thermalize much more slowly than light partons. If charm quarks are observed to have sizable collective motion, then light partons, which dominate the medium, should be fully thermalized. The charm quark flow can be measured through open [17] and closed charm particles. The J/ψ is the most prominent for experiment among the latter. However, because the J/ψ production mechanism is not well understood, there is significant uncertainty associated with this probe, since only J/ψ from recombination of charm quarks inherit their flow. A detailed comparison between experimental measurements and models on J/ψ v_2 vs. transverse momentum (p_T) and centrality, in

addition to nuclear modification factor, will shed light on the J/ψ production mechanism and charm quark flow.

This analysis benefits from a large amount of data taken during the RHIC [18] $\sqrt{s_{NN}} = 200$ GeV Au+Au run in the year 2010 by the new data acquisition system of STAR [19], capable of an event rate up to 1 kHz. In addition, the newly installed Time Of Flight (TOF) detector [20] allows STAR to improve electron identification, and background electrons from photon conversion are reduced by one order of magnitude due to less material around the center of the detector setup.

The data presented consist of 360 million minimum bias (MB) events triggered by the coincidence of two Vertex Position Detectors [21], 270 million central events triggered by a large hit multiplicity in the TOF detector [20], and a set of high tower events triggered by signals in the towers of Barrel Electromagnetic Calorimeter (BEMC) [22] exceeding certain thresholds (2.6, 3.5, 4.2, and 5.9 GeV). The high tower sample is equivalent to approximately 7 billion MB events for J/ψ production in the high- p_T region. In addition, in order to cope with the large data volume coming from collisions at high luminosity, a High Level Trigger (HLT) was implemented to reconstruct charged tracks online, select events with J/ψ candidates and tag them for fast analysis. There are 16 million J/ψ enriched events selected by the HLT.

The J/ψ were reconstructed through the $J/\psi \rightarrow e^+e^-$ channel, with a branching ratio of 5.9 %. The daughter tracks of the J/ψ were required to have more than 20 hits in the Time Projection Chamber (TPC) [23], and a distance of closest approach less than 1 cm from the primary vertex. Low momentum electrons and positrons can be separated from hadrons by selecting on the inverse velocity ($0.97 < 1/\beta < 1.03$), which is calculated from the time-of-flight measured by the TOF detector [20] and the path length measured by the TPC. At large momentum ($p > 1.5$ GeV/c), with the energy measured by towers from the BEMC [22], a cut of the momentum to energy ratio ($0.3 < p/E < 1.5$) was applied to select electrons and positrons. The electrons and positrons were then identified by their specific energy loss per unit track length ($\langle dE/dx \rangle$) inside the TPC. More than 15 TPC hits were required to calculate $\langle dE/dx \rangle$. The $\langle dE/dx \rangle$ cut is asymmetric around the expected value for electron, because the lower side is where the hadron $\langle dE/dx \rangle$ lies. It also varies according to whether the candidate track passes the $1/\beta$ and/or p/E cut to optimize efficiency and purity. The combination of cuts on $1/\beta$, p/E and $\langle dE/dx \rangle$ enables electron/positron identification in a wide momentum range. Our measured J/ψ particles cover the rapidity range $-1 < y < 1$, favoring J/ψ near

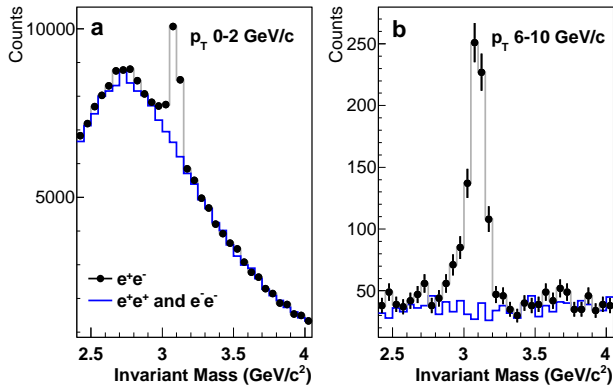


FIG. 1. (color online) Invariant mass spectrum of elec-
 tron/positron pairs for $0 < p_T < 2$ GeV/c (a) and $6 < p_T <$
 10 GeV/c (b). The points are unlike-sign pairs with the J/ψ
 signal. The blue solid line histogram shows the like-sign back-
 ground.

$y = 0$ because of detection efficiency variation due to
 acceptance and decay kinematics.

A total of just over 13000 J/ψ were reconstructed in
 the entire p_T range of 0-10 GeV/c, and the invariant mass
 spectra of e^+e^- pairs with the J/ψ signals for the lowest
 (0-2 GeV/c) and highest (6-10 GeV/c) p_T bins are shown
 in Fig. 1.

The following method has been used to calculate the
 v_2 of J/ψ . Firstly, measurements of $\phi - \Psi$, ranging from
 0 to π , were divided into 10 bins. Here ϕ is the az-
 imuthal angle of J/ψ , and Ψ is the azimuthal angle of
 the event plane reconstructed from TPC tracks with the
 azimuthally nonuniform detector efficiency corrected [24].
 Then two bins at supplementary angles were combined
 into one. The J/ψ yield within a combined $\phi - \Psi$ bin
 was obtained by fitting the e^+e^- pair invariant mass dis-
 tribution with a Gaussian signal on top of a second order
 polynomial background. Then v_2 was obtained by fit-
 ting the J/ψ yield vs. $\phi - \Psi$ with a functional form of
 $A(1 + 2v_2 \cos(2(\phi - \Psi)))$. Finally, the observed v_2 was
 corrected for the event plane resolution [24].

Three dominant sources of systematic error have been
 investigated for this measurement: assumptions in the
 calculation method, hadron contamination for the daugh-
 ter e^+e^- pairs, and the non-flow effect. The first source
 can be estimated from the difference in v_2 calculated by
 methods with different assumptions. Two other meth-
 ods are used here. One is similar to the original method,
 except that the J/ψ yield in each combined $\phi - \Psi$ bin
 was not obtained from fitting, but from subtracting the
 like-sign background from unlike-sign distribution within
 the possible invariant mass range of J/ψ . In the other
 method, the overall v_2 of both signal and background
 was measured first as a function of invariant mass, and
 then it was fitted with an average of J/ψ v_2 and back-

ground v_2 weighted by their respective yields vs. invari-
 ant mass [25]. The systematic error from hadron con-
 tamination can be estimated from the difference in cal-
 culated v_2 with different electron/positron identifica-
 tion cuts. While the original cuts aim for the best J/ψ
 signal, a purer electron/positron sample can be obtained
 from a set of tighter cuts. The overall systematic uncer-
 tainty for the first two sources was estimated from the maxi-
 mum difference between the calculated v_2 with the 3×2
 $= 6$ combinations of v_2 methods and electron/positron
 identification cut sets mentioned above. Besides elliptic
 flow, there are also some other two- and many-particle
 correlations due to, for example, resonance decay and
 jet production. These non-flow correlations may influ-
 ence the reconstructed event plane and the measured v_2 .
 To estimate this non-flow influence on the v_2 measure-
 ment, a method of scaling non-flow in $p + p$ collisions
 to that in Au + Au collisions [26] was employed. This
 method assumes that 1) J/ψ -hadron correlation in $p +$
 p collisions is entirely due to non-flow, and 2) the non-
 flow correlation to other particles per J/ψ in Au + Au
 collisions is similar to that in $p + p$ collisions. Under
 these assumptions, it can be deduced that the non-flow
 influence on measured J/ψ v_2 in Au+Au collisions is
 $\langle \sum_i \cos 2(\phi_{J/\psi} - \phi_i) \rangle / M \overline{v_2}$. Here the sum is over hadrons
 and the average is over J/ψ in $p + p$ collisions. M and
 $\overline{v_2}$ are the multiplicity and average elliptic flow of hadrons
 in Au+Au collisions, respectively. Since the away side
 correlation may be greatly modified by the medium in
 heavy-ion collisions, this procedure gives an upper limit
 of the non-flow effect. Detector acceptance and efficiency
 variation with p_T , centrality and rapidity may lead to a
 biased J/ψ sample, which may induce some systematic
 effects when v_2 also changes with these parameters. But
 these effects are estimated to be negligible compared to
 statistical errors.

Figure 2 shows J/ψ v_2 as a function of transverse mo-
 mentum for different centralities, with the estimation of
 non-flow shown by the lines. Data from the central trig-
 ger, minimum bias trigger and high tower triggers are
 used for the 0-10 % most central bin, while only mini-
 mum bias and high tower triggered events are used for
 other centrality bins. Considering errors and the magni-
 tude of non-flow, J/ψ v_2 is consistent with 0 for $p_T >$
 2 GeV/c for all measured centrality bins. Light particles
 usually have a larger v_2 in the intermediate centrality
 than in the most central and peripheral collisions. This
 can be explained by a larger initial spatial eccentricity in
 the intermediate centrality, which is transferred into fi-
 nal state momentum anisotropy due to different pressure
 gradients in different directions, when there are sufficient
 interactions in the medium. However, no strong cen-
 trality dependence for J/ψ v_2 has been observed in our
 measurement.

The top panel of Fig. 3 shows J/ψ v_2 for 0 - 80 %

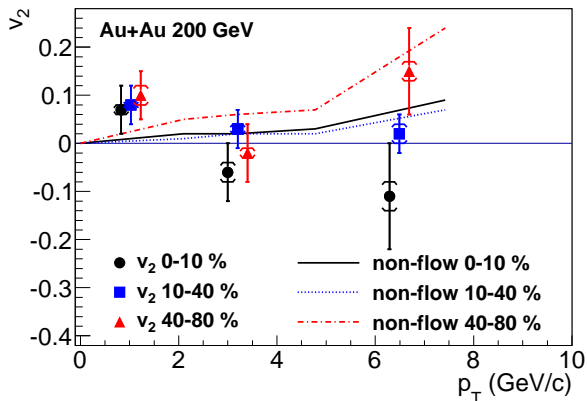


FIG. 2. (color online) v_2 vs. p_T for J/ψ in different centrality bins. The brackets represent systematic errors estimated from differences between different methods and cuts. The p_T bins for J/ψ are 0-2, 2-5 and 5-10 GeV/c. The mean p_T in each bin for the J/ψ sample used for v_2 calculation is drawn, but is shifted a little for some centralities so that all points can be seen clearly. The curves show estimated non-flow influence on measured v_2 (see text).

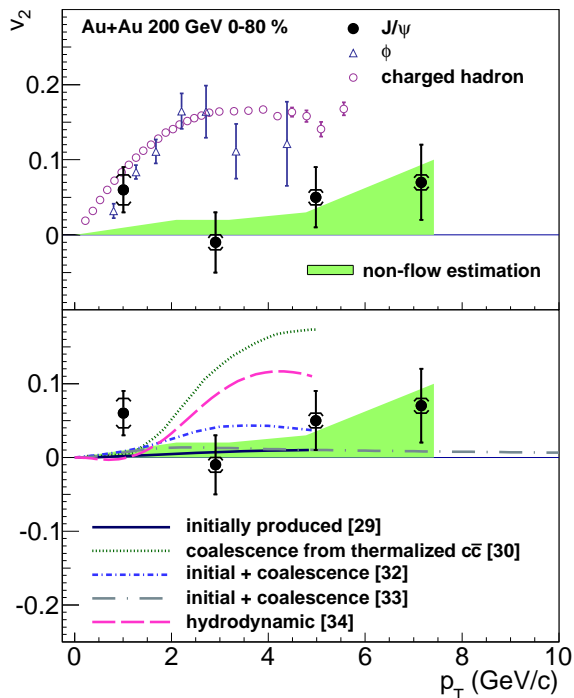


FIG. 3. (color online) v_2 vs. p_T for J/ψ in 0-80% central events comparing with charged hadrons [27] and the ϕ meson [28] (upper panel) and theoretical calculations [29–34] (lower panel). The brackets represent systematic errors estimated from differences between different methods and cuts. The p_T bins for J/ψ are 0-2, 2-4, 4-6 and 6-10 GeV/c, and the mean p_T in each bin for the J/ψ sample used for v_2 calculation is drawn. Estimated non-flow influence on measured v_2 is shown as the shaded band.

central collisions as a function of transverse momentum. For reference, two other sets of v_2 measurements are also plotted, one is for charged hadrons (dominated by pions) [27] and the other is for the ϕ meson [28] which is heavier than the pion but not as heavy as the J/ψ . Unlike v_2 of hadrons consisting of light quarks, J/ψ v_2 at $p_T > 2$ GeV/c is found to be consistent with zero within statistical errors. However, the significant mass difference between J/ψ and light particles makes the direct comparison of v_2 vs. p_T less conclusive. For example, for the same velocity at $y = 0$, the p_T of J/ψ at 3.0 GeV/c corresponds to p_T of pions (ϕ) at 0.14 (1.0) GeV/c.

In the bottom panel of Fig. 3, a comparison is made between the measured J/ψ v_2 and various theoretical calculations, and a quantitative level of difference is shown in Table I by χ^2/NDF and the p-value. v_2 of J/ψ produced by initial pQCD processes is predicted to stay close to zero [29]. Although both normal suppression due to nuclear absorption and anomalous suppression in the hot medium due to color screening are considered in the model, the azimuthally different suppression along the different path lengths in azimuth leads to a limited v_2 beyond the sensitivity of the current measurement. On the contrary, if charm quarks get fully thermalized and J/ψ are produced by coalescence from the thermalized flowing charm quarks at the freeze-out, the v_2 of J/ψ is predicted to reach almost the same maximum magnitude as v_2 of light flavor mesons, although at a larger p_T (around 4 GeV/c) due to the significantly larger mass of J/ψ [30]. This is 3σ above the measurement for $p_T > 2$ GeV/c, leading to a large χ^2/NDF of 21.1/3 and a small p-value of 1.0×10^{-4} , and is thus inconsistent with the data. Models that include J/ψ from both initial production and coalescence production in the transport model [29, 31] predict a much smaller v_2 [32, 33], and are consistent with our measurement. In these models, J/ψ are formed continuously through the system evolution rather than at the freeze-out, so many J/ψ could be formed from charm quarks whose v_2 has still not fully developed. Furthermore, the initial production of J/ψ with very limited v_2 dominates at high p_T , thus the overall J/ψ v_2 does not rise rapidly as for light hadrons. This kind of model also describes the measured J/ψ nuclear modification factor over a wide range of p_T and centrality [5]. The hydrody-

TABLE I. Difference between model calculations and data. The p-value is the probability of observing a χ^2 that exceeds the current measured χ^2 by chance, even for a correct model.

theoretical calculation	χ^2/NDF	p-value
initially produced [29]	3.7 / 3	2.9×10^{-1}
coalescence from thermalized $c\bar{c}$ [30]	21.1 / 3	1.0×10^{-4}
initial + coalescence [32]	3.7 / 3	3.0×10^{-1}
initial + coalescence [33]	4.9 / 4	3.0×10^{-1}
hydrodynamic [34]	10.1 / 3	1.7×10^{-2}

237 namic model, which assumes local thermal equilibrium,²⁷²
 238 can be tuned to describe v_2 for light hadrons, but it pre-²⁷³
 239 dicts a J/ψ v_2 that rises strongly with p_T in the region²⁷⁴
 240 $p_T < 4$ GeV/ c , and thus fails to describe the main fea-²⁷⁵
 241 ture of the data [34]. For heavy particles such as J/ψ ,²⁷⁶
 242 hydrodynamic predictions suffer from large uncertainties²⁷⁷
 243 related to viscous corrections (δf) at freeze-out and the²⁷⁸
 244 assumed freeze-out time or temperature.²⁷⁹

245 In summary, J/ψ elliptic flow is presented as a func-²⁸¹
 246 tion of transverse momentum for different centralities in,²⁸²
 247 $\sqrt{s_{NN}} = 200$ GeV Au+Au collisions. Unlike light flavor²⁸³
 248 hadrons, J/ψ v_2 at $p_T > 2$ GeV/ c is consistent with zero²⁸⁴
 249 within statistical errors. Comparing to model calcula-²⁸⁵
 250 tions, the measured J/ψ v_2 values disfavor the scenario²⁸⁶
 251 that J/ψ with $p_T > 2$ GeV/ c are produced dominantly²⁸⁷
 252 by coalescence from (anti-)charm quarks which are ther-²⁸⁸
 253 malized and flow with the medium.²⁸⁹

254 We thank the RHIC Operations Group and RCF at²⁹²
 255 BNL, the NERSC Center at LBNL and the Open Science²⁹³
 256 Grid consortium for providing resources and support.²⁹⁴
 257 This work was supported in part by the Offices of NP²⁹⁵
 258 and HEP within the U.S. DOE Office of Science, the U.S.²⁹⁶
 259 NSF, the Sloan Foundation, CNRS/IN2P3, FAPESP²⁹⁷
 260 CNPq of Brazil, Ministry of Ed. and Sci. of the Russian²⁹⁸
 261 Federation, NNSFC, CAS, MoST, and MoE of China,²⁹⁹
 262 GA and MSMT of the Czech Republic, FOM and NWO³⁰⁰
 263 of the Netherlands, DAE, DST, and CSIR of India, Pol-³⁰¹
 264 ish Ministry of Sci. and Higher Ed., National Research³⁰²
 265 Foundation (NRF-2012004024), Ministry of Sci., Ed. and³⁰³
 266 Sports of the Rep. of Croatia, and RosAtom of Russia.³⁰⁴

-
- 267 [1] T. Matsui and H. Satz, Phys. Lett. B **178**, 416 (1986).³¹¹
 268 [2] M. C. Abreu *et al.*, Phys. Lett. B **499**, 85 (2001).³¹²
 269 [3] A. Adare *et al.*, Phys. Rev. Lett. **98**, 232301 (2007).³¹³
 270 [4] A. Adare *et al.*, Phys. Rev. C **77**, 024912 (2008).³¹⁴
 271 [5] L. Adamczyk *et al.*, e-print arXiv:1208.2736 (2012).³¹⁵

- [6] B. Abelev *et al.*, Phys. Rev. Lett. **109**, 072301 (2012).
 [7] M. B. Johnson *et al.*, Phys. Rev. Lett. **86**, 4483 (2001).
 [8] V. Guzey, M. Strikman, and W. Vogelsang, Phys. Lett. B **603**, 173 (2004).
 [9] R. Baier, D. Schiff, and B. G. Zakharov, Ann. Rev. Nucl. Part. Sci. **50**, 37 (2000).
 [10] S. Gavin and R. Vogt, Nucl. Phys. A **610**, 442C (1996).
 [11] R. L. Thews, Eur. Phys. J. C **43**, 97 (2005).
 [12] R. L. Thews and M. L. Mangano, Phys. Rev. C **73**, 014904 (2006).
 [13] A. Andronic, P. Braun-Munzinger, K. Redlich, and J. Stachel, Nucl. Phys. A **789**, 334 (2007).
 [14] A. Capella *et al.*, Eur. Phys. J. C **58**, 437 (2008).
 [15] P. F. Kolb and U. W. Heinz, in *Quark Gluon Plasma*, edited by R. C. Hwa and X. N. Wang (World Scientific, Singapore, 2003) pp. 634–714.
 [16] P. Huovinen and P. V. Ruuskanen, Ann. Rev. Nucl. Part. Sci. **56**, 163 (2006).
 [17] S. S. Adler *et al.*, Phys. Rev. C **72**, 024901 (2005).
 [18] H. Hahn *et al.*, Nucl. Instrum. Meth. A **499**, 245 (2003).
 [19] K. H. Ackermann *et al.*, Nucl. Instrum. Meth. A **499**, 624 (2003).
 [20] B. Bonner *et al.*, Nucl. Instrum. Meth. A **508**, 181 (2003).
 [21] W. J. Llope *et al.*, Nucl. Instrum. Meth. A **522**, 252 (2004).
 [22] M. Beddo *et al.*, Nucl. Instrum. Meth. A **499**, 725 (2003).
 [23] M. Anderson *et al.*, Nucl. Instrum. Meth. A **499**, 659 (2003).
 [24] A. M. Poskanzer and S. A. Voloshin, Phys. Rev. C **58**, 1671 (1998).
 [25] N. Borghini and J. Y. Ollitrault, Phys. Rev. C **70**, 064905 (2004).
 [26] J. Adams *et al.*, Phys. Rev. Lett. **93**, 252301 (2004).
 [27] J. Adams *et al.*, Phys. Rev. Lett. **92**, 062301 (2004).
 [28] B. I. Abelev *et al.*, Phys. Rev. Lett. **99**, 112301 (2007).
 [29] L. Yan, P. Zhuang, and N. Xu, Phys. Rev. Lett. **97**, 232301 (2006).
 [30] V. Greco, C. M. Ko, and R. Rapp, Phys. Lett. B **595**, 202 (2004).
 [31] L. Ravagli and R. Rapp, Phys. Lett. B **655**, 126 (2007).
 [32] X. Zhao and R. Rapp, e-print arXiv:0806.1239 (2008).
 [33] Y. Liu, N. Xu, and P. Zhuang, Nucl. Phys. A **834**, 317c (2010).
 [34] U. W. Heinz and C. Shen, private communication (2011).